Proceedings of the 11th ICPMG 2026
11th International Conference on Physical Modelling in Geotechnics
8-12 June 2026, Zurich, Switzerland

Centrifuge modelling of shear wave velocity evolution in sandy foundation during seismic loading

Q. Ma, Y. Zhou, Y. Cao, X. Zhang, Z. Yan
MOE Key Laboratory of Soft Soils and Geoenvironmental Engineering, Institute of Hypergravity Science and Technology, Zhejiang University, Hangzhou, P.R. China, ma_qiang@zju.edu.cn, qzking@zju.edu.cn, Yuancao13@zju.edu.cn, 3210103548@zju.edu.cn, yanzizhuang@zju.edu.cn

ABSTRACT: Earthquake records have shown that shear wave velocity of a site can drop abruptly during shaking and then recover through rapid and gradual phases. But centrifuge tests often struggle to capture this process due to compressed time scales. In this study, a real-time shear wave velocity testing system was used to monitor shear wave velocity of a silty sand foundation under different shaking intensities. Results show different evolution patterns between small and large shaking events. Under small shaking, shear wave velocity recovers as excess pore water pressure dissipated, yielding a post-shaking shear wave velocity greater than the initial value. In contrast, under strong shaking, the shear wave velocity reappeared at approximately 37% of its pre-shaking value and then increased to reach the pre-shaking level as the foundation consolidated. Despite further densification during reconsolidation, the shear wave velocity did not exceed its pre-shaking value. These findings provide direct experimental evidence of the transient loss and staged recovery of shear wave velocity in liquefied soils.

1 INTRODUCTION

Shear wave velocity is a fundamental parameter for characterizing soil stiffness and seismic response. Observations from numerous earthquake events have shown that, under seismic loading, the shear wave velocity of a site can drop abruptly and subsequently recover through both rapid and gradual phases (Pavlenko, 2002; Sawazaki et al., 2006; Wang et al., 2021). A comprehensive understanding of soil stiffness degradation and recovery during earthquakes is therefore essential for improving the accuracy of site seismic response analyses and post-earthquake foundation performance assessments.

Centrifuge model tests are among the most effective approaches for investigating the degradation and recovery of site stiffness under seismic loading. However, due to the compressed time scales inherent in centrifuge testing, capturing the real-time evolution of shear wave velocity during shaking remains a significant challenge. Traditional centrifuge bender element testing systems (Fu et al., 2004; Zhou et al., 2010), which rely on oscilloscopes for data acquisition, typically require several minutes to complete a single measurement. As a result, shear wave velocity can usually only be obtained before and after shaking, making it difficult to monitor the transient stiffness changes occurring during seismic events. Some recent studies have attempted to address this limitation by monitoring shear wave velocity during shaking (e.g., Lee et al., 2012; Ma et al., 2025), but experimental evidence capturing the full degradation and recovery process remains limited.

In this study, centrifuge shaking table tests were conducted at 50 *g* on an embankment foundation system. Both small and strong shaking motions were applied to investigate the evolution of excess pore water pressure and shear wave velocity at the base of the embankment under different shaking intensities. The results show that seismic loading induced a rapid increase in excess pore water pressure, leading to foundation softening and a pronounced reduction in shear wave velocity, followed by gradual post-shaking recovery. Under small shaking, the post-shaking shear wave velocity slightly exceeded its pre-shaking value, whereas under strong shaking, the shear wave velocity recovered to approximately its pre-shaking level. These results provide new experimental insight into the transient degradation and staged recovery of soil stiffness during and after seismic loading.

2 CENTRIFUGE MODEL TESTS

2.1 Testing apparatus

The centrifuge shaking table model tests were conducted using the ZJU-400 geotechnical centrifuge at Zhejiang University. The centrifuge has a radius of 4.5 m, a maximum centrifugal acceleration of 150 *g*, and a maximum effective payload capacity of 400 *g*·t. The centrifuge is equipped with an in-flight shaking table for applying seismic loading. The main technical specifications of the shaking table include a maximum vibration acceleration of 40 *g*, an operating frequency range from 10 Hz to 200 Hz, a maximum horizontal velocity of 1 m/s, and a maximum horizontal displacement of ± 6 mm. A rigid model container was adopted, with the internal dimensions of the model box are 770 mm in length, 400 mm in width, and 530 mm in height. Further details of the ZJU-400 centrifuge and the in-flight shaking table can be found in Zhou et al. (2018).

The shear wave velocity of the model was monitored using the real-time shear wave velocity testing system developed by Ma et al. (2025). A key advantage of this system is its capability to continuously track the evolution of shear wave velocity during the post-earthquake pore pressure dissipation process within the model.

2.2 Model preparation

As illustrated in Figure 1, the centrifuge model consists of an embankment–foundation system. At the model scale, a 2 cm thick non-liquefiable dense Ottawa F65 sand layer with a relative density of 90% was placed at the bottom. Above this layer, an intermediate layer composed of Ottawa F65 sand mixed with 10% silt, with a relative density of 83%, was prepared. The top layer consists of a 1 cm thick Fujian coarse sand layer with a relative density of 70%. An embankment with a height of 12 cm was constructed on the foundation soil, with side slopes of 1:1.5. The particle size distributions of Ottawa F65 sand, silt, and Fujian coarse sand are presented in Figure 2, while the basic physical properties of these materials are summarized in Table 1.

Arrays of accelerometers and pore pressure transducers were installed beneath the embankment, with a vertical spacing of 6 cm between sensors in each layer. Two pairs of bender elements were embedded at depths of 7 cm and 19 cm to measure the shear wave velocity of the model. The distances between transmitter and receiver were 10.30 cm for BE1 and 9.78 cm for BE2. A laser displacement sensor was installed at the crest of the embankment to monitor embankment settlement during shaking.

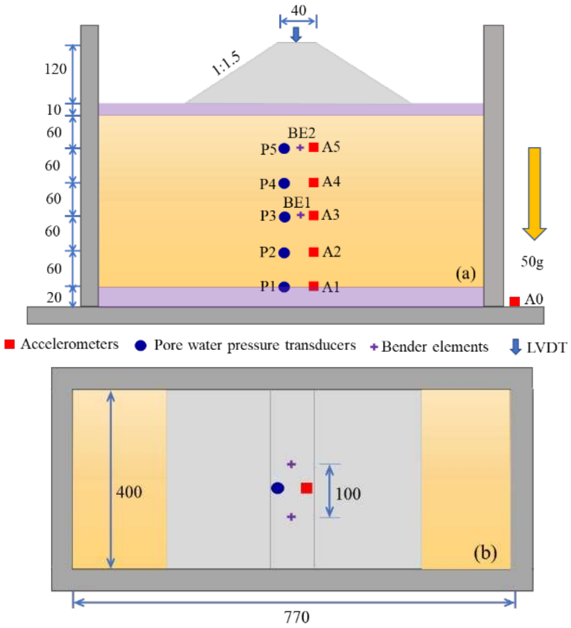

Figure 1. Centrifuge model instrumentations (Unite: mm)

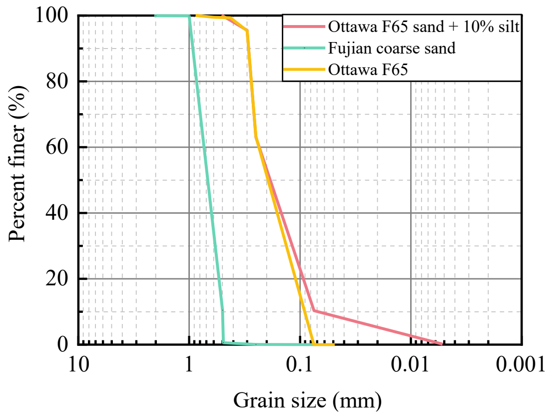

Figure 2. Grain size distribution of model soil

Table 1. Physical properties of model soil

Soil	Specific gravity (-)	Min. density (g/cm^3)	Max. density (g/cm^3)
Ottawa F65	2.665	1.475	1.756
Ottawa F65 + 10% silt	2.673	1.510	1.921
Fujian coarse sand	2.644	1.489	1.713

The model was prepared using the air pluviation method. After preparation, the model was saturated with a 50 cSt methyl silicone oil solution under a vacuum pressure of approximately −90 kPa.

2.3 Test procedure and motion sequence

After completing the model preparation, the centrifuge was incrementally accelerated in steps of 10 *g* until reaching the target centrifugal acceleration of 50 *g*. At each acceleration level, shear wave velocity tests were conducted once the pore water pressure and embankment crest settlement had stabilized.

Following the shear wave velocity measurements, the model was subjected to two sinusoidal input motions with a prototype frequency of 1 Hz, with peak ground acceleration (PGA) amplitudes of 0.1 *g* and 0.25 g, respectively.

3 TEST RESULTS AND DISCUSSION

3.1 V_s measurements using BE tests at various *g*-levels

Figure 3 shows the relationship between shear wave velocity and mean effective stress of the model at different centrifugal accelerations, where the mean effective stress was estimated through the finite element method. At 50 *g*, the mean effective stresses at BE1 and BE2 are approximately 102 kPa and 75 kPa, respectively. The results indicate that the shear wave velocity of the model increases nonlinearly with increasing mean effective stress, following a power-law relationship. This trend can be well fitted using Eq. (1), proposed by Hardin and Richart (1963):

$$V_s = Af(e)(\sigma_m)^{\frac{n}{2}} = \alpha(\sigma_m)^{\beta} \quad (1)$$

where A and n are best-fit parameters that capture the effects of soil fabric and stress conditions; and $f(e)$ is a function of void ratio e. In this study, $\alpha = 68.5$, $\beta = 0.25$.

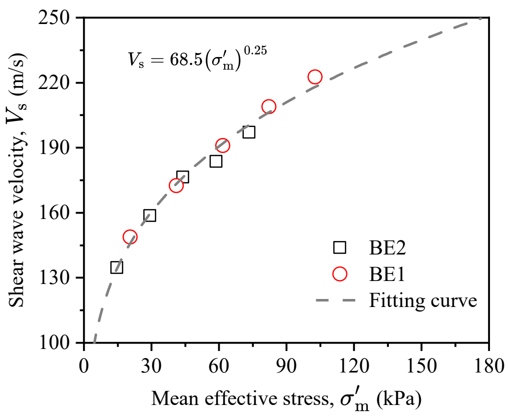

Figure 3. Shear wave velocity versus mean effective stress at different g level

3.2 Excess pore water pressure and shear wave velocity

Figure 4 presents the time histories of excess pore water pressure (EPWP) measured at P5 and shear wave velocity monitored by BE2 under a PGA of 0.1 *g*. The excess pore water pressure rose to a maximum of approximately 15 kPa during shaking and gradually dissipated afterward. The shear wave velocity remained around 200 m/s prior to shaking. During the shaking, the bender elements were affected by the intense vibrations generated by the shaking table, resulting in malfunction and an inability to capture meaningful changes in shear wave velocity. Following the shaking, as the excess pore water pressure dissipated, the foundation gradually consolidated, and the shear wave velocity increased from 156 m/s to 206 m/s. The apparent stepwise variation in V_s is caused by the measurement resolution of approximately 3 m/s. Ultimately, the post-shaking shear wave velocity was approximately 3% higher than the pre-shaking value.

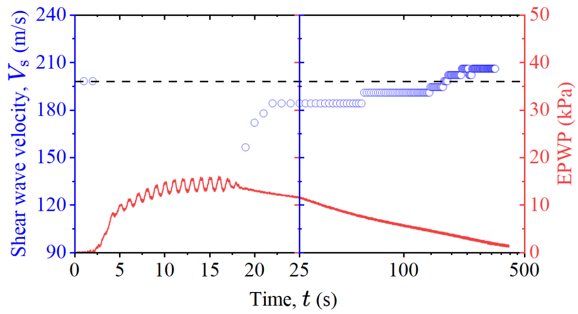

Figure 4. The variation of excess pore water pressure (EPWP) and shear wave velocity under PGA=0.1g

Figure 5 shows the time histories of excess pore water pressure measured at P5 and shear wave velocity monitored by BE2 under a PGA of 0.25 *g*. In contrast to Figure 4, the stronger shaking induced significant softening of the foundation, with the shear wave velocity decreasing from 206 m/s to 78 m/s, representing a reduction of 63%. Subsequently, as the excess pore water pressure dissipated, the shear wave velocity gradually recovered to its pre-shaking level.

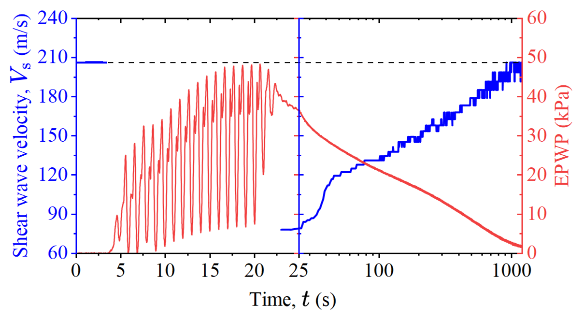

Figure 5. The variation of excess pore water pressure (EPWP) and shear wave velocity under PGA=0.25g

3.3 Settlements

Figure 6 shows the crest settlement of the embankment during the two shaking events, which were 0.05 m and 0.34 m, respectively. According to Eq. (1), the settlement of the foundation leads to an increase in void ratio, which would be expected to result in a corresponding increase in post-shaking shear wave velocity. The measured data indicate that after the minor shaking with PGA = 0.1 *g*, the foundation shear wave velocity increased slightly. In contrast, following the major shaking with PGA = 0.25 *g*, although the foundation void ratio increased, the shear wave velocity did not show a significant change. This behavior may be attributed to the strong shaking damaging the structural and fabric characteristics of the soil, leading to a considerable reduction in the parameter A in Eq. (1), such that the post-shaking shear wave velocity remained comparable to its pre-shaking value.

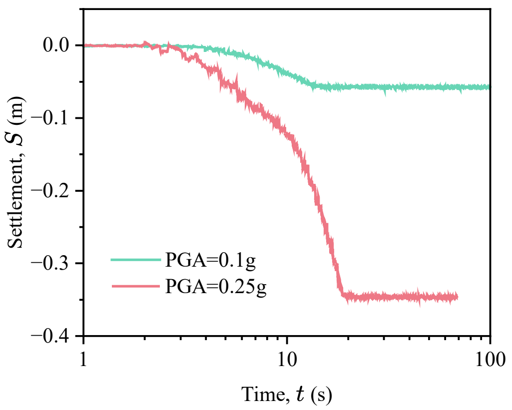

Figure 6. The settlement of the embankment crest

4 CONCLUSIONS

This study conducted a centrifuge shaking table test on an embankment founded on silt–sand soil under 50 *g* to investigate the evolution of shear wave velocity before and after seismic loading. The results indicated that:

(1) Under small seismic loading, the shear wave velocity recovered as excess pore water pressure dissipated. Subsequent reconsolidation further densified the soil, resulting in a post-shaking shear wave velocity approximately 3% higher than its initial value.

(2) After strong seismic loading, the foundation softened due to the development of high excess pore water pressure, and the shear wave velocity reappeared at approximately 37% of its pre-shaking value before increasing to reach its pre-shaking level as the foundation consolidated. Despite an increase in the foundation void ratio inferred from post-shaking settlements, no significant increase in shear wave velocity was observed after strong shaking. This behavior was likely attributed to the degradation of soil structure and fabric caused by intense seismic loading, which counteracted the effect of reconsolidation on shear wave velocity.

ACKNOWLEDGEMENTS

This study was supported by the National Natural Science Foundation of China (Nos. 52408400, 52588202, and 52278374) and the National Key R&D Program of China (2024YFF 1702003).

REFERENCES

Hardin B.O. and Richart F.E. (1963). Elastic wave velocities in granular soils. *Journal of Soil Mechanics and Foundations Division, ASCE*, 89(SM1): 39–56. https://doi.org/10.1061/JSFEAQ.0000493

Lee C.J., Wang C.R., Wei Y.C. and Hung W.Y. (2012). Evolution of the shear wave velocity during shaking modeled in centrifuge shaking table tests. *Bulletin of Earthquake Engineering*, 10(2): 401–420. https://doi.org/10.1007/s10518-011-9314-y

Ma Q., Zhou Y.G., Yan Z.Z., Chen Y.M. Development of a real-time shear wave velocity testing system for centrifuge model tests. *International Journal of Physical Modelling in Geotechnics*, 12(1): 2500028. https://doi.org/10.1680/jphmg.25.00028

Pavlenko O. (2002). Changes in shear moduli of liquefied and nonliquefied soils during the 1995 Kobe Earthquake and its aftershocks at three vertical-array sites. *Bulletin of the Seismological Society of America*, 92(5): 1952–1969. https://doi.org/10.1785/0120010143

Sawazaki K., Sato H., Nakahara H. and Nishimura T. (2006). Temporal change in site response caused by earthquake strong motion as revealed from coda spectral ratio measurement. *Geophysical Research Letters*, 33(21): L21303. https://doi.org/10.1029/2006GL027938

Wang S.Y., Zhuang H.Y., Zhang H. et al. (2021). Near-surface softening and healing in eastern Honshu associated with the 2011 magnitude-9 Tohoku-Oki Earthquake. *Nature Communications*, 12(1): 1215. https://doi.org/10.1038/s41467-021-21418-7

Zhou Y.G., Sun Z.B., Chen Y. M. (2018). Zhejiang University benchmark centrifuge test for LEAP-GWU-2015 and liquefaction responses of a sloping ground. *Soil Dynamics and Earthquake Engineering*, 113: 698–713. http://dx.doi.org/10.1016/j.soildyn.2017.03.010